THz quantum cascade lasers in magnetic fields

© V.I. Gavrilenko[1,2], D.I. Kuritsyn[1], M.A. Fadeev[1], A.V. Antonov[1], A.A. Yantser[1,2], K.A. Kovalevsky[1], S.V. Morozov[1,2], A.A. Dubinov[1,2], R.Kh. Zhukavin[1]

[1] Institute for Physics of Microstructures,
603087 Afonino, Kstovsky district, Nizhny Novgorod region, Russia
[2] Lobachevsky State University,
603022 Nizhny Novgorod, Russia

E-mail: gavr@ipmras.ru

Received April 15, 2024
Revised June 20, 2024
Accepted June 20, 2024

The current-voltage and emission characteristics of quantum cascade lasers of the range 3.3−3.7 THz, manufactured in Russia, were measured in magnetic fields up to 5 Tesla at helium temperature. When a magnetic field was applied, a decrease in threshold currents and a narrowing of the zone of intense generation from high currents side were observed. In the dependences of the radiation intensity on the magnetic field, a characteristic minimum was observed in magnetic fields in which the doubled cyclotron energy is compared with the energy of the radiation quantum, which indicates the inclusion of resonant scattering when the 2nd Landau level, related to the lower laser level, crosses the zero Landau level, related to the upper laser one.

Keywords: quantum cascade laser, terahertz range, current-voltage characteristic, emission characteristic, magnetic field, Fourier-transform spectroscopy.

DOI: 10.61011/SC.2024.04.58847.6347H

1. Introduction

A quantum cascade laser (QCL) is a semiconductor heterosystem with a large (up to several hundred) number of tunnel-coupled quantum wells (QW); generation takes place due to induced electron transitions between levels of dimensional quantization in QW when an external electric field is applied [1,2]. Currently, QCL are compact, efficient semiconductor radiation sources in the mid-infrared (IR) and terahertz (THz) ranges. These devices can operate continuously at room temperature in the middle IR range, and the radiation power can exceed 1 W [3]. The approach developed during creation of QCL emitting in the middle IR range was also used for THz (far-IR) QCL, first implemented in 2002 [4]. Various designs of the QCL active region are known, of which the most effective are designs with a superlattice active region, in which transitions from bound state to free state (bound-to-continuum) [5] are used for photon emission, and a scheme containing several QW in the active region with population inversion based on the rapid emptying of the lower operating level due to the resonant emission of a longitudinal optical phonon [6]. The highest achieved operating temperatures in the THz frequency range are 261 K with pulsed pumping [7]. The QCL radiation power in the 3 THz frequency range reaches 230 mW in continuous mode [8] and several Watts in pulse mode [9], however, the output power and operating temperatures significantly decrease in case of transition from 3 to 1 THz due to various physical limitations. First of all, this is attributable to the fact that the value of the energy gap between the operating levels (~ 8 meV for a frequency of 2 THz) becomes comparable with the energy broadening of the subbands (units of meV). At the same time, the efficiency of electron injection to the upper laser level decreases. The operating range of THz QCL is limited on the high-frequency side (from 3 to 5 THz) by the Reststrahlen band in GaAs — a material on the basis of which almost all known QCL of this range are currently produced. There is a fairly old conference report from the Japanese group [10] about the creation of 5 and 7 THz QCL based on GaN/AlGaN, but there is no journal publication of this result. This paper does not provide information about the output power, however, it corresponds to the microwatt level judging by the signal-to-noise ratio on the given spectra.

The application of a strong magnetic field normal to the layers of the QCL structure results in two types of effects. Firstly, the „zero dimensionality“ of the electronic spectrum results in the suppression of parasitic scattering and a decrease of the threshold currents of the QCL. Secondly, magnetic quantization results in an oscillating (in case of magnetic field sweep) dependence of the lifetime at the upper laser level, which causes an oscillating dependence of the intensity of laser radiation on the magnetic field (sometimes outwardly resembling the Shubnikov−de Haas oscillations). Such effects were observed for the first time in the QCL of the middle IR range in pulsed magnetic fields up to 60 T, while the intensity of the QCL radiation was many times higher at the oscillation maxima than the signal at $B = 0$ [11,12].

The first study of the effects of the magnetic field in the THz QCL was carried out a year after its creation. A sample made of the same structure as the first THz QCL [13] was studied (see also [14]). In contrast to the mid-IR QCL,

where any noticeable effects were observed in the fields over 10 T, a pronounced oscillating dependence of the radiation intensity on the magnetic field was already observed in THz QCL in permanent magnetic fields up to 6 T. The lower state of each level of dimensional quantization in case of application of a magnetic field is shifted upwards by $\hbar\omega_c/2$, where $\hbar$ is Planck's constant, and $\omega_c = eB/m^*c$ is the cyclotron frequency of the electron. Here e — electron charge, c — speed of light, $m^* = 0.069m_0$ — effective electron mass in GaAs QW [13], m_0 — the mass of a free electron. „Critical“ is the value of the magnetic field at which the nth Landau level related to the lower operating level of the QCL, intersects with the zero Landau level, related to the upper laser level. Despite the fact that these states are orthogonal, such an intersection results in the resonant transitions between these states due to various scattering mechanisms: interfaces, impurities, acoustic phonons, electron-electron scattering. As a result, electrons from the upper (pumped) laser level are scattered to the nth Landau level of the lower laser level and then relax in a non-radiative manner. Therefore, the population inversion drops, which manifests itself in an increase of threshold current and a drop of radiated power.

Similar studies were carried out in subsequent years in Ref. [15–17], which confirmed the oscillating nature of the characteristics of the QCL versus the magnetic field. The range of stationary magnetic fields in which the study was conducted was expanded to 12 T in Ref. [16] and to 26 T in [17]. The emission spectra of QCL in magnetic fields were also measured in these studies, and the switching of generation to neighboring modes of the Fabry-Perot resonator was demonstrated. In the general case, generation can occur at transitions between different subbands when more levels of dimensional quantization are involved in electronic transport. For instance, generation was observed at a frequency of 1.38 THz at transitions between levels 3 and 2 in a wide QW in a strong magnetic field of 11.5 T at low currents in Ref. [18,19], and switching to a frequency of 2.3 THz occurred at transitions between levels 4 and 3 at high currents. The paper [20] first studied THz QCL with the „resonant-phonon“ design of the active region that was also used in the QCL studied in this paper. The structure was designed to generate radiation in the range of 3 THz (at $B = 0$) and was studied in stationary magnetic fields up to 31 T. The „switching“ of generation to transitions between other operating levels and tuning of the radiation frequency from 3 THz to the region of 0.7–1 THz was demonstrated in this paper, in addition to the increase of the output power and reduction of the threshold current in case of application of a magnetic field over 16 T. A similar result of „switching“ of generation from 3 THz to the range of 0.7–1.4 THz in significantly more accessible magnetic fields of up to 8–10 T at low temperatures was obtained in Ref. [21] in a structure with „stepped“ QW is in the active region. Finally, it is necessary to note the paper [22], in which a two-frequency generation near 3.4 and 3.8 THz was observed in a QCL with a „resonant phonon“ design with 3 QW GaAs/AlGaAs for a period, while the introduction of a magnetic field up to 8 T smoothly shifted the center of gravity of the spectrum into the high-frequency region. In conclusion of the review, it is necessary to note that studies of oscillations of QCL characteristics in a magnetic field were not carried out during the above studies of QCL with a „resonant-phonon“ design.

2. Experiment procedure

The studied QCL were processed into structures with a double metal waveguide (DMW). The post-growth technology of fabricating the strip lasers with the Au–Au DMW is described in detail in Ref. [23]. The characteristic width of the strip was 100 μm. The strip lasers were formed by cleaving, the strip length was 1–3 mm. Due to the high reflectance of terahertz radiation from the cleaved faces, $R \sim 80$–85%, a strong feedback occurs in the longitudinal direction of the laser strips, which forms the Fabry-Perot resonator. The cleaved strip THz QCLs were mounted on „C-mount“ heat sinks; the electrical contact was made by welding several golden wires of the 30 μm, diameter to the upper strip, while those wires are uniformly distributed along the entire length of the strip.

The studied QCL was placed in a liquid helium cryostat directly in liquid helium ($T = 4.2$ K) in the center of a superconducting solenoid. The magnetic field was directed perpendicular to the layers of the structure (parallel to the current) so that the direction of the laser radiation output was perpendicular to the magnetic field (in the horizontal direction). The radiation was directed using a mirror upward in a waveguide made of a polished stainless steel tube with a diameter of 18 mm. The measurements were carried out in pulse mode (pulse duration 1–2 μs, repetition rate 100–200 Hz). The structures were powered using a specially fabricated electronic key, which allows producing the pulses of a given duration, off-duty ratio and amplitude, as well as measuring the voltage and current passing through the laser. The radiation was detected by an impurity photodetector Ge : Ga inserted from above into the cryostat waveguide in case of measurement of the dependences of the integral intensity of the QCL radiation on the pumping current (L–I-characteristics) or on the magnetic field (L–B-characteristics). The photodetector was located at a sufficient distance from the end of the superconducting solenoid to exclude the influence of a scattered magnetic field on its sensitivity (which was verified by an independent experiment). Signals proportional to the amplitude of the voltage, current and signal pulses from the detector were recorded by a 4-channel digital oscilloscope Tektronics TDS 3034 and were saved in the computer memory during automatic scanning in case of measurements of the current-voltage curve (I–V characteristics) and the integral dependences of the QCL radiation on current or magnetic field. A digital signal from the superconducting solenoid power supply was also recorded in the computer memory during the magnetic field sweep. The typical maximum

radiation power was several milliwatts. Radiation was introduced using a rotary mirror into BRUKER Vertex 80v Fourier spectrometer operating in step-by-step scanning mode for studying the spectra of QCL radiation in magnetic fields. The radiation from the output of the spectrometer was introduced over a similar waveguide from a stainless steel tube was introduced into Dewar transport helium vessel STG-40, where it was detected by the same impurity photodetector Ge : Ga.

3. Results and discussion

Figure 1 shows the results of studies of QCL № 1 with „resonant phonon“ design of the active region with three QW in the cascade. The structure was grown by molecular beam epitaxy (MBE), the results of the study of this QCL in a zero magnetic field are presented in Ref. [24]. Generation was observed at modes 2−3 of the Fabry-Perot resonator with a central frequency of ~ 3.3 THz. The figure shows that the characteristic features on the $I-V$ curve near 2.8−3.2 A and 3.6−4.2 A coincide with the beginning and end of the region of intense generation at all magnetic fields. At the moment of laser generation, the rate of current growth with voltage increases, which is associated with a decrease of the lifetime of electrons at the upper laser level. Such an effect of stimulated optical transitions on electronic transport indicates a sufficiently high quantum efficiency of the device. On the contrary, „switching off“ of stimulated radiation results in a slowdown of the growth of current with voltage. Figure 1 shows that the application of a magnetic field results in a shift of both the features associated with laser generation on the $I-V$ curve and the generation zone to the region of lower currents. The decrease of the threshold current with an increase of the magnetic field is obviously attributable to the „zero dimensionality“ of states, which results in the suppression of parasitic scattering and an increase of the lifetime of carriers at the upper laser level. The narrowing of the zone of intensive generation from high currents is most likely attributable to a decrease of the broadening of the upper laser level and a faster (compared with the case of $B = 0$) mismatch with the level of the injector with an increase of current and, accordingly, voltage at the cascade.

Similar results were obtained in the study of QCL № 2 with 3 QW in a cascade made of a heterostructure also grown by the MBE method according to the design described in [25], where the radiation frequency was 3.9 THz, and generation was observed up to $T = 186$ K. In our case, the frequency of the main mode was 4.08 THz, and not 3.9 THz, as in Ref. [25].

Figure 2 shows the results of studies of QCL № 2 in magnetic fields up to 5 T. Characteristic features are observed on the $I-V$ curve corresponding to the currents at which generation begins and subsides as in the case of QCL № 1. Just as in the previous case, the application of a magnetic field results in a shift of both the features on the

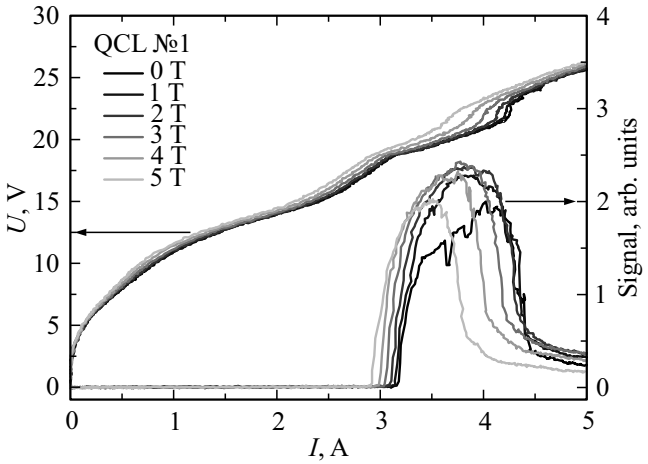

Figure 1. $I-V$ and $L-I$-characteristics of QCL № 1 in magnetic fields from 0 to 5 T. (A color version of the figure is provided in the online version of the paper).

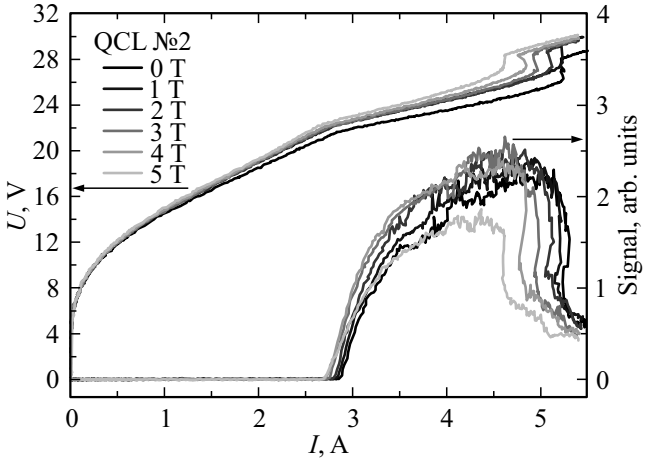

Figure 2. $I-V$ and $L-I$-characteristics of QCL № 2 in magnetic fields from 0 to 5 T.

$I-V$ curve and the generation zone to the region of lower currents, i.e., to a decrease of the threshold current.

Let us now proceed to the description of the results of the study of QCL with a 4-well design. The structures of these lasers were designed in such a way as to allow the emission of two photons when an electron passes through one cascade of the structure [26,27]. An intermediate/middle (m) level is placed between the upper (u) and the lower (l) working levels in such a „two-photon“ design, so that the population inversion between the upper and lower levels is „exchanged“ for two laser transitions: $u \to m$ and $m \to l$. In the more general case, 4 radiative transitions are possible when the operating levels and the injector (i) and the extractor (e) levels are not completely aligned: $u \to m$, $i \to m$, $m \to l$ and $m \to e$. The heterostructures of QCL № 3 and № 4 were grown by chemical vapor deposition technique [28]. Calculations of the band structure and gain spectra in linear and nonlinear modes performed according

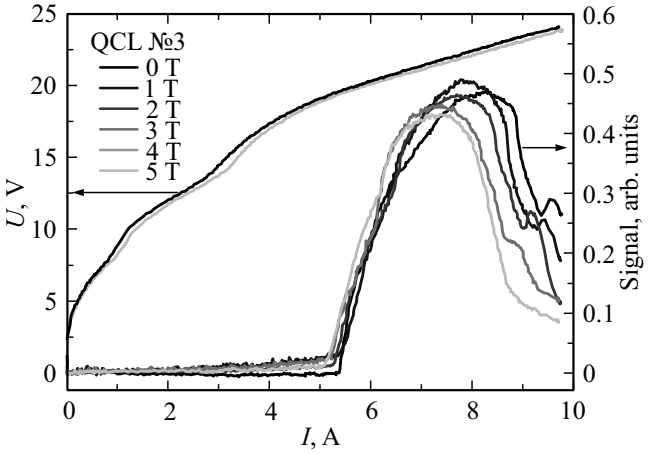

Figure 3. $I-V$ and $L-I$-characteristics of QCL № 3 in magnetic fields from 0 to 5 T.

to the methodology developed in [29] showed that the gain in the heterostructure of QCL № 3 at an operating voltage at the cascade (67.0 mV) occurs at transitions between the levels of the injector and the middle level ($i \to m$) and from the middle to the lower laser level ($m \to l$) that have frequencies of ~ 3.7 THz. The level u in case of such shift is above the level of the injector i and its population is small. A high-frequency peak (4.46 THz) in the gain spectrum suppressed in the nonlinear mode due to the dominance of generation at the low-frequency peak corresponds to $u \to m$ transition. As will be shown below, generation in QCL No 3 is indeed observed at a frequency of 3.7 THz.

Figure 3 shows the results of studies of QCL № 3 in magnetic fields up to 5 T. Unlike the QCL № 1 and № 2 described above, the $I-V$ curve of QCL № 3 has no features in the field of currents from 5.2 to 10 A corresponding to the generation zone. At the same time, as in previous cases, the threshold current slightly decreases when a magnetic field is applied, and a noticeable drop of the intensity of generation on the high current side was also observed when a magnetic field was applied.

Figure 4 shows the dependences of the radiation intensity on the magnetic field QCL № 3 and № 4 at different current values. The calculated gain spectrum of QCL № 4 contains two maxima at frequencies 2.8 and 3.9 THz corresponding to the transitions $m \to l$ and $u \to m$, respectively. The frequency of the most intense mode was 3.8THz in the experiment, which is close to the calculated value of 3.9THz for transitions to the middle level m. Low-frequency generation near 2.8 THz was not observed at transitions from the middle level. Figure 4, *a, b* shows that a pronounced minimum of the intensity of QCL radiation is observed in the same magnetic field of $B = 4.7$ T in both cases, with almost all currents. The corresponding cyclotron energy value is

$$\hbar\omega_c = heB/m^*c = 7.85\,\text{meV}.$$

The doubled value of the cyclotron energy $2\hbar\omega_c = 15.7$ meV coincides with the quantum energy corresponding to the position of the main line in the radiation spectrum of QCL № 4 (3.8 THz, 15.7 meV) and is close (taking into account the minimum width at $B = 4.7$ T in Figure 4, *a*) to the quantum energy corresponding to the position of the main line in the radiation spectrum of QCL № 3 (3.7THz, 15.3 meV). Thus, this minimum can be confidently associated with the intersection of the 2nd Landau level from the lower operating levels of the QCL for the observed transitions with zero Landau levels of the upper operating levels, leading to resonance scattering and a decrease of the populations of the upper laser levels (cf. with data from [13]).

Figure 5 shows the emission spectra of QCL № 2 (with 3 QW in the cascade) and № 3 (with 4 QW in the cascade), measured with a resolution of 1 cm^{-1} in a zero magnetic field and in magnetic fields of 3 and 5 T. As can be seen from the figure, the application of a magnetic

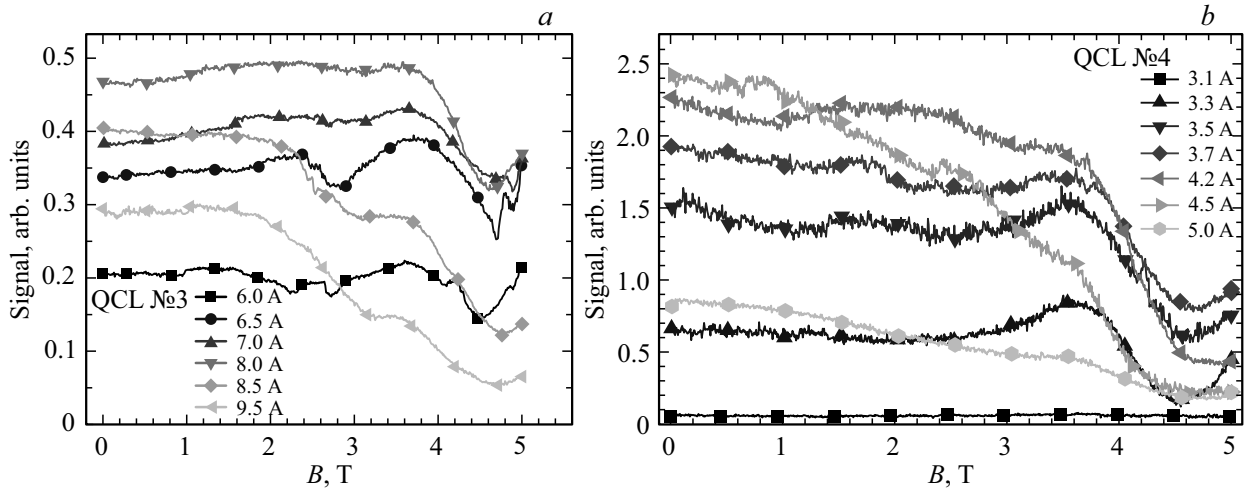

Figure 4. $L-B$-characteristics of QCL № 3 (*a*) and № 4 (*b*) at different current values.

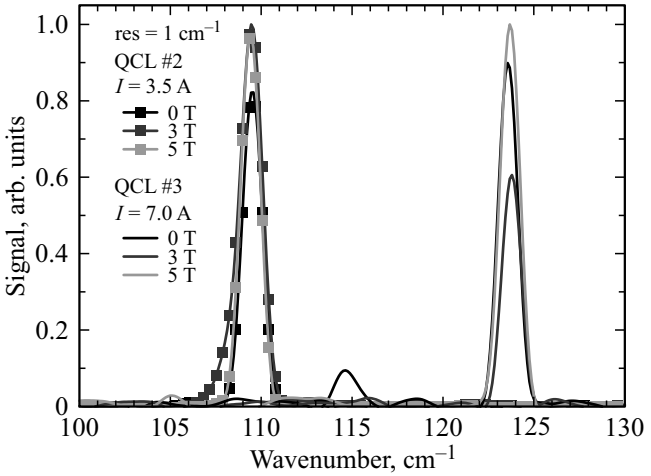

Figure 5. Emission spectra of QCL № 2 ($I = 3.5$ A) and № 3 ($I = 7.0$ A) in a zero magnetic field and in fields of 3 and 5 T, measured with spectral resolution of 1 cm^{-1}.

field up to 5 T does not result in a tuning of the radiation spectrum — generation occurs at the same transitions as with $B = 0$ in contrast to the paper [18–22], where switching of generation to lower frequency transitions was observed in stronger magnetic fields of 8–30 T.

4. Conclusion

A study of the current-voltage ($I-V$) and radiative ($L-I$) characteristics at helium temperature of terahertz QCL, produced in Russia, showed that the application of a magnetic field results in a decrease of threshold currents due to the zero dimensionality of states and a decrease of parasitic scattering. A narrowing of the zone of intensive generation was also observed on the side of high currents when a field was applied, which may also be associated with a narrowing of the upper laser level in the magnetic field and its mismatch with the level of the injector with an increase of current/voltage. For a QCL with a „resonant-phonon“ design (the lower laser level is emptied due to the resonant emission of an optical phonon), a characteristic minimum was observed for the first time in the dependence of the radiation intensity on the magnetic field in which the doubled cyclotron energy is compared with the energy of the radiation quantum, which suggests the inclusion of resonant scattering at the intersection of 2-the Landau level related to the lower laser level, with the zero Landau level related to the upper laser level.

Funding

The work was supported by the NCFM (project „Studies in strong and super-strong magnetic fields“ — studies of $I-V$, $L-I$- and $L-B$-characteristics of QCL) and a grant from the Russian Science Foundation No. 23-19-00436 (measurement radiation spectra of QCL).

Acknowledgments

The authors would like to thank A.A. Afonenko, D.V. Ushakov and R.A. Khabibullin for useful discussions of the results of the work.

Conflict of interest

The authors declare that they have no conflict of interest.

References

[1] M.S. Vitiello, G. Scalari, B. Williams, P. De Natale. Opt. Express, **23**, 5167 (2015).
[2] M.S. Vitiello, A. Tredicucci. Adv. Phys.: X, **6**, 1893809 (2021)
[3] Y. Bai, S.R. Darvish, S. Slivken, W. Zhang, A. Evans, J. Nguyen, M. Razeghi. Appl. Phys. Lett., **92**, 101105 (2008).
[4] R. Köhler, A. Tredicucci, F. Beltram, H.E. Beere, E.H. Linfield, A.G. Davies, D.A. Ritchie, R.C. Iotti, F. Rossi. Nature, **417**, 156 (2002).
[5] L. Ajili, G. Scalari, J. Faist, H. Beere, E. Linfield, D. Ritchie, G. Davies. Appl. Phys. Lett., **85**, 3986 (2004).
[6] B.S. Williams. Nature Photonics, **1**, 517 (2007).
[7] A. Khalatpour, M. C. Tam, S. J. Addamane, J. Reno, Z. Wasilewski, Q. Hu. Appl. Phys. Lett., **122**, 161101 (2023).
[8] X. Wang, C. Shen, T. Jiang, Zh. Zhan, Q. Deng, W. Li, W. Wu, N. Yang, W. Chu, S. Duan. AIP Advances, **6**, 075210 (2016).
[9] Y. Jin, J.L. Reno, S. Kumar. Optica, **7**, 708 (2020).
[10] W. Terashima, H. Hirayama. Proc. SPIE, **9483**, 948304 (2015).
[11] C. Becker, C. Sirtori, O. Drachenko, V. Rylkov, D. Smirnov, J. Leotin. Appl. Phys. Lett., **81**, 2941 (2002).
[12] D. Smirnov, C. Becker, O. Drachenko, V.V. Rylkov, H. Page, J. Leotin, C. Sirtori. Phys. Rev. B, **66**, 121305(R) (2002).
[13] J. Alton, S. Barbieri, J. Fowler, H.E. Beere, J. Muscat, E.H. Linfield, D.A. Ritchie, G. Davies, R. Kö hler, A. Tredicucci. Phys. Rev. B, **68**, 081303R (2003).
[14] G. Scalari, S. Blaser, L. Ajili, J. Faist, H. Beere, E. Linfield, D. Ritchie, G. Davies. Appl. Phys. Lett., **83**, 3453 (2003).
[15] V. Tamosiunas, R. Zobl, G. Fasching, J. Ulrich, G. Strasser, K. Unterrainer, R. Colombelli, C. Gmachl, K. West, L. Pfeiffer, F. Capasso. Semicond. Sci. Technol., **19**, S348 (2004).
[16] G. Scalari, S. Blaser, J. Faist, H. Beere, E. Linfield, D. Ritchie, G. Davies. Phys. Rev. Lett., **93**, 237403 (2004).
[17] G. Scalari, C. Walther, L. Sirigu, M.L. Sadowski, H. Beere, D. Ritchie, N. Hoyler, M. Giovannini, J. Faist. Phys. Rev. B, **76**, 115305 (2007).
[18] G. Scalari, C. Walther, J. Faist, H. Beere, D. Ritchie. Appl. Phys. Lett., **88**, 141102 (2006).
[19] G. Scalari, C. Walther, M. Fischer, R. Terazzi, H. Beere, D. Ritchie, J. Faist. Laser & Photon. Rev., **3**, 45 (2009).
[20] A. Wade, G. Fedorov, D. Smirnov, S. Kumar, B.S. Williams, Q. Hu, J.L. Reno. Nature Photonics, **3**, 41 (2009).
[21] G. Scalari, D. Turčinková, J. Lloyd-Hughes, M.I. Amanti, M. Fischer, M. Beck. Appl. Phys. Lett., **97**, 081110 (2010).
[22] M.A. Kainz, S. Schönhuber, B. Limbacher, A.M. Andrews, H. Detz, G. Strasser, G. Bastard, K. Unterrainer. Appl. Phys. Lett., **114**, 191104 (2019).
[23] N.V. Shchavruk, A.Yu. Pavlov, D.S. Ponomarev, K.N. Tomosh, R.R. Galiev, P.P. Maltsev, A.E. Zhukov, G.E. Tsyrlin, F.I. Zubov, J.I. Alferov. FTP, **50**, 1395 (2016). (in Russian).

[24] R.A. Khabibullin, K.V. Maremyanin, D.S. Ponomarev, R.R. Galiev, A.A. Zaitsev, A.I. Danilov, I.S. Vasilevsky, A.N. Vinnichenko, A.N. Klochkov, A.A. Afonenko, D.V. Ushakov, S.V. Morozov, V.I. Gavrilenko. FTP, Semiconductors, **56**, 71 (2022).
[25] S. Kumar, Q. Hu, J.L. Reno. Appl. Phys. Lett., **94**, 131105 (2009).
[26] V.I. Gavrilenko. In: Proc. Russian conf. On actual problems of semicond. photoelectronics (Photonics 2023), September 4–8, 2023, Novosibirsk, Russia, ISBN 978-5-00218-581-8, p. 26
[27] M.A. Talukder, P. Dean, E.H. Linfield, A.G. Davies. Opt. Express, **30**, 31785 (2022).
[28] T.A. Bagaev, M.A. Ladugin, A.A. Marmalyuk, A.I. Danilov, D.V. Ushakov, A.A. Afonenko, A.A. Zaitsev, K.V. Maremyanin, S.V. Morozov, V.I. Gavrilenko, R.R. Galiev, A.Yu. Pavlov, S.S. Pushkarev, D.S. Ponomarev, R.A.Khabibullin. Pis'ma ZhTF, **48** (10), 16 (2022). (in Russian).
[29] D.V. Ushakov, A.A. Afonenko, A.A. Dubinov, V.I. Gavrilenko, O.Yu. Volkov, N.V. Shchavruk, D.S. Ponomarev, R.A. Khabibullin. Quantum Electronics, **49**, 913 (2019).

Translated by A.Akhtyamov